SEVENTH QUARTERLY REPORT
ON

"SPECTRORADIOMETRIC CALIBRATION OF THE THEMATIC MAPPER AND MULTISPECTRAL SCANNER SYSTEM"

Contract Number NAS5-27382
For the Period: 1 May 1984 - 1 August 1984

NASA/Goddard Space Flight Center
Greenbelt MD 20771

James M. Palmer, Co-Investigator
Philip N. Slater, Principal Investigator

Optical Sciences Center
University of Arizona
Tucson, Arizona 85721

INTRODUCTION

This is the seventh quarterly report on Contract NAS5-27382 entitled, "Spectroradiometric Calibration of the Thematic Mapper and the Multispectral Scanner System." In this report, we summarize the reduction of the data measured on July 8, 1984 at White Sands, New Mexico. The radiances incident at the entrance pupil of the Landsat 5 sensors have been computed for bands 1-4. When these are compared to the digital counts of the TM image, we will have the ground based calibration of this sensor. The image has been received from Goddard SFC and is presently being analyzed.

JULY 8, 1984 CALIBRATION

Field Measurements

This was our first opportunity to acquire on-site measurements at White Sands in conjuction with Thematic Mapper imagery from Landsat 5. Imagery was not available for previous trips due to cloud cover. Assisting in the field measurements were Harumi Aoki, Ken Castle, Barbara Capron, Madgeleine Dinguirard, Ron Holm, Ray Jackson, Carol Kastner, Amy Phillips, Rich Savage, and Phil Slater. The instrumentation on hand included two Barnes radiometers, the cart and yoke, an old model of Reagan's radiometer, both of the Castle spectropolarimeters, four polycorders, a printer, the Compaq computer, and two 2 X 2 ft standard reflectance panels.

Sunrise on the morning of July 8th was at 6:10 a.m. New Mexico was on Mountain Daylight Time (MDT) this time of year, as are the times quoted here. The Reagan instrument was set up and began acquiring solar irradiance measurements at 7:15 a.m. (airmass 4). Rich Savage took temperature, humidity, and pressure readings there at Chuck site. He also arranged for a nearby radiosonde ascent. These data are presented in Appendix B.

Two test sites had been laid out on the previous trip. Each was a 4 X 4 pixel grid, aligned with the east/west scan lines expected of Landsat. A road with a 120° bend separated the two sites, and will facilitate the identification of the sites on the digital TM imagery. Each site was measured with a Barnes radiometer. Starting at the center of

each 30 X 30 meter pixel, five reflectance measurements were taken of the gypsum sands, within an area of about 5. X 0.5 meters. Reflectance panel readings were taken periodically during the course of these measurements. (Both the $BaSO_4$ and Halon panels were recalibrated by Che Nianzeng immediately upon our return.) The data were averaged and recorded on polycorders. The site to the North of the road was scanned using the Purdue radiometer (one of the Barnes), mounted on the cart with the $BaSO_4$ panel. Data were taken from 11 to 11:20 a.m. The south site was scanned simultaneously with an USDA Barnes attached to a yoke. A Halon panel was used as the reference here. In addition to the two 4 X 4 pixel areas, two small areas were scanned near the van. This was done between 10:20 and 11:40 a.m. These areas were selected for their contrast, representing extremes of light and dark for the local area. They will later be used in conjunction with aerial photography to map the reflectance of the entire area. Finally, diffuse to direct measurements were taken between 8:30 and 10:20 a.m. These were made by comparing the radiance reflected from the ground to that radiance measured when the sun was blocked with a styrofoam parasol. These data can be used for comparison with the radiative transfer code, to verify our atmospheric models.

A helicopter overflight was arranged for this trip. Jack Rees and co-pilot Keys piloted the helicopter and Jason Penny, PFC, was the photographer. The flight was almost exactly one full hour. It had the dual purpose of recording radiance at intermediate altitudes, again for comparison to the radiative transfer code output, and photographing the sites. Several slides have been scanned, using a microdensitometer, and will be used to characterize the ground reflectance. Five rolls of

Ektachrome, ASA 100, were shot. All photos were taken at 1/500th of a second, with a 200 mm focal length lens. A series were taken at 6,000, 2,000, and 500 ft., AGL (above ground level). The photos were bracketed from F/16 to F/22, in half F/stop increments. Those taken at 2,000 ft. were particulary suited to our needs. Eight colored ground cloths had been laid out to define the two 4 X 4 pixel areas that were measured with the Barnes. We noted that the blue and orange ground cloths were the most visible from the air, as well as being the easiest to see on the color slides.

The field tests of the newly constructed spectropolarimeters will have to wait for our next trip to White Sands. The helicopter instrument suffered from a power failure, and data from the ground instrument, used for solar irradiance measurements, were lost during the TRS-80 to Compaq transfer. Back-up equipment was, however, available that enabled us to conduct an approximate calibration described in the following.

Langley Plot Computations

The Reagan radiometer was cycled through its narrowband filter set 95 times during the course of the morning. Each data set included, to the nearest second, a start and finish time and a voltage reading for each of the 9 spectral filters. These data were used as input to a program which computed solar zenith angle from ephemermis data. Using a refraction correction, airmasses were then calculated for each measurement. Finally, a weighted least squares analysis was used to compute the slope of the natural log voltages versus airmass, at each wavelength. The computed slopes are equivalent to the spectral optical depths of the atmosphere, τ_{ext}, at the time of overpass. Temporal

stability of the atmosphere is assumed. These results are given in Table 1. Also shown are the optical depth components τ_{Mie}, τ_{Ray}, and τ_{oz}. The computation of these components is discussed next.

Using measured atmospheric pressure (883 mbar), τ_{Ray} can be easily computed. After subtracting this from τ_{ext}, a curve is plotted, as in Figure 1a, which contains only Mie and ozone components. To determine τ_{Mie} a curve is fit through all the $\tau_{ext}-\tau_{Ray}$ data points that do not include absorption. Normally this is done by submitting the optical depth values to a routine which fits the data to an equation of the form $\log \tau_{Mie}=a_0+a_1 \log \lambda + a_2(\log \lambda)^2$. As many of the spectral filter data sets were rejected, an alternate approach was taken here. These problems arose because the older of the two Reagan radiometers was used. On this instrument the heater was not functioning. The data are less reliable without the temperature stabilization, due to fluctuations in detector responsitivity. This problem is thought to have affected mainly the 0.872 and 1.03 μm channels.

Instead of our normal procedures, therefore, a manual fitting of the data was performed. A curve of the form $\log \tau_{Mie}=a_0+a_1 \log \lambda$ was assumed (a straight line on this log-log plot). This is an approximation, valid only if the aerosols can be correctly modeled as obeying a Junge radial size distribution, $dn/dr=c\, r^{-(\nu+1)}$. In such a case the data would fall exactly on a line whose slope, a_1, yields the Junge parameter ν via the relationship $a_1=-\nu+2$. By using only the 0.440 and 0.780 μm data points, a slope was determined. At these wavelengths the ozone absorption coefficients are small. Actually, the 0.440 and 0.872 μm pair is prefered, as the absorption coefficients are approximately equal. The

Table 1. Langley Plot Results.

Data from Reagan Radiometer
8 July, 1984
Chuck Site, White Sands, New Mexico

Latitude	32.935°
Longtitude	106.407°
Right Ascension	7.226228 hours
Declination	22.365361°
Difference (Dec)	-419.3 arc-sec
Earth-Sun Distance	1.016701 AU
Pressure	883. mbar

WAV(μm)	τ_{ext}	τ_{Mie}	τ_{Ray}	τ_{oz}
0.4000	0.4426	0.0981	0.3172	0.0000
0.4400	0.3060	0.0922	0.2138	0.0006
0.5217	0.1921	0.0824	0.1063	0.0127
0.6120	0.1543	0.0743	0.0555	0.0246
0.6708	0.1091	0.0699	0.0382	0.0098
0.7120	0.1063	0.0673	0.0300	0.0046
0.7797	0.0842	0.0634	0.0208	0.0027
0.8717	0.0948	0.0589	0.0133	0.0006
1.0303	0.1103	0.0528	0.0068	0.0000

$\log \tau_{Mie} = a_0 + a_1 \log \lambda$; λ in μm
$a_0 = -1.269$ $a_1 = -0.654$

$$\tau_{Ray} = \frac{29123.7\ (n^2-1)^2}{\lambda^4}$$

$$n = 6432.8 + \frac{2949810}{146-\lambda^2} + \frac{25540}{41-\lambda^4}$$

λ in micrometers

$\tau_{oz,\lambda} = NOZ * \alpha_\lambda$
NOZ = columnar ozone

$$= \frac{\tau_{oz,0.612\ \mu m}}{\alpha_{0.612\ \mu m}} = 213.2 \text{ matm-cm}$$

α = spectral absorption coefficient

Table 2. Spectral components for TM midband wavelengths.

WAV (μm)	τ_{ext}	τ_{Mie}	τ_{Ray}	τ_{oz}	E_0(mW/cm²)
0.486	0.2339	0.0864	0.1421	0.0055	175.955
0.571	0.1745	0.0777	0.0735	0.0232	180.580
0.661	0.1226	0.0706	0.0406	0.0114	153.916
0.838	0.0773	0.0605	0.0156	0.0013	104.708

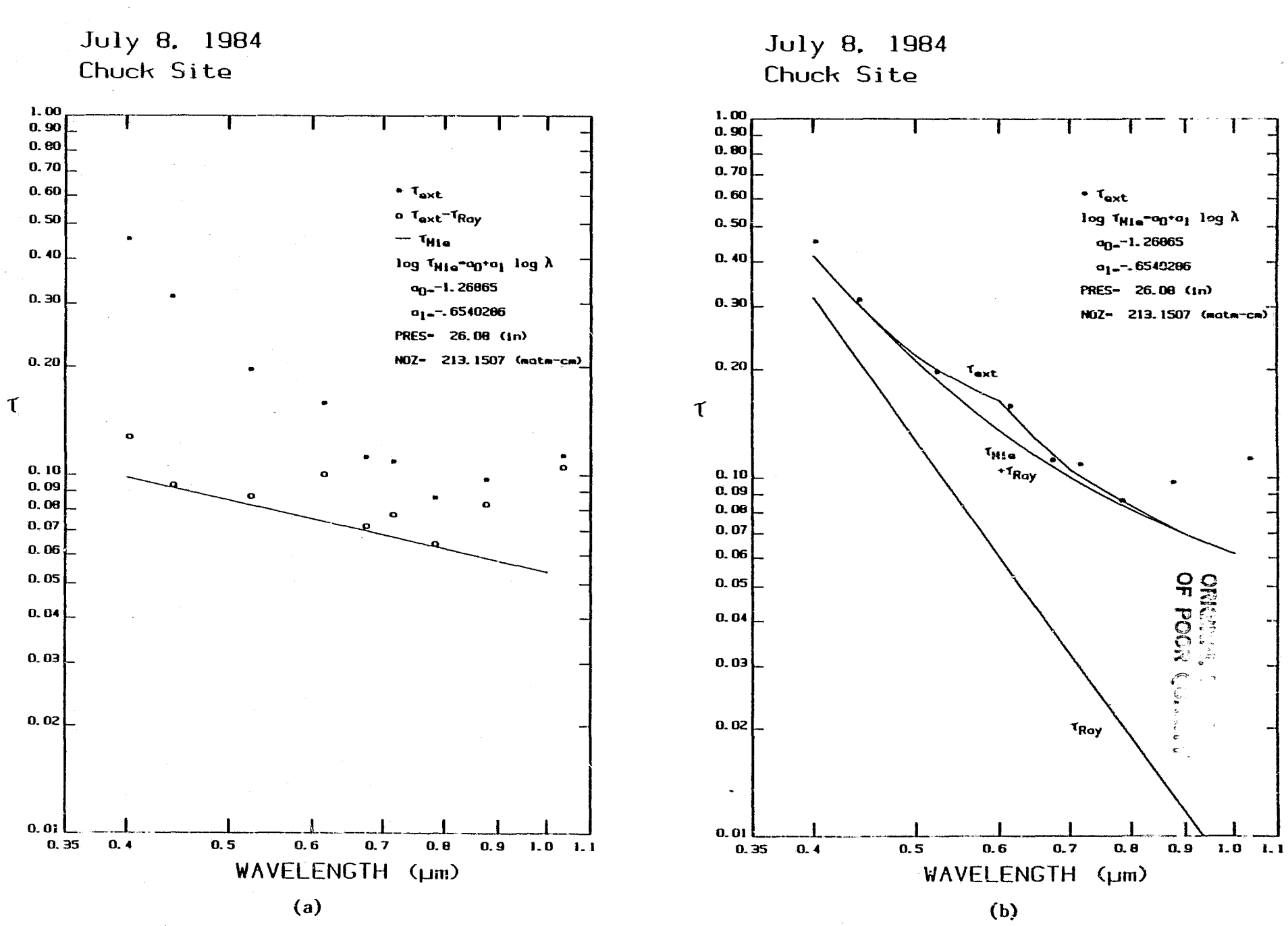

Figure 1. Optical depth versus wavelength data from the Reagan radiometer.

data at 0.872 μm for this date, however, is unreliable, due to the temperature problem mentioned above. With the given constraints, the slope was found to be a_1=-0.654, thus ν=2.65, and a_0=-1.269. With these constants the τ_{Mie}, τ_{Ray}, and τ_{oz} components can be computed for any wavelength. Figure 1b shows how each of these components contributes to the total optical depth. Table 2 gives the respective components for the TM midband wavelengths. These data will be used as input to the radiative transfer code. To be complete, a component of τ_{H2O} should be included for band 4. The contribution due to water vapor has not as yet been assessed. Also reported is the exo-atmospheric solar irradiance, as determined from interpolating the data of Neckel and Labs (1981). The midband wavelengths of the TM sensor was computed by Palmer (1984) using the moments method and the pre-flight filter transmittance data.

Panel Calibration

The Herman radiative transfer code requires that the absolute reflectance of the gypsum sands be known. We have instead chosen to use the reflectance factor $R(\theta_z/0°)$. (A discussion of reflectance nomenclature and definitions is given in Appendix A.) Here θ_z is the angle incident upon the gyspum, and 0° is the reflected angle, equal to the Thematic Mapper nadir-look angle. By using this quantity, the amount of light reflected in the direction of the TM is accurately characterized. A full BRDF characterization would be prefered. The gain in accuracy is not warranted, however, as the BRDF data would be difficult and time consuming to obtain.

In the field the reflectance factor is measured with one of two Barnes radiometers. As these are uncalibrated they must be used in

conjunction with a reference panel. The reflectance factor of the sands is determined via the relationship

$$R_{sand} = \frac{V_{sand} * R_{ref}}{V_{ref}} . \qquad (1)$$

Here V_{sand} and V_{ref} are the output voltages of the Barnes when looking over the sands and reference panel, respectively. These voltages are proportional to the radiance scattered upward and within the instrument's 15° field of view (FOV). R_{ref} is the reflectance factor of the panel, as determined in the laboratory. On July 8th one of the radiometers was assigned the Halon panel; the other radiometer was assigned the $BaSO_4$ panel. While looking at the sands, each Barnes was periodically swung over the reference panel and voltage readings were recorded. Upon our return Che Nianzeng calibrated both panels.

The calibration of the panels was conducted at the Optical Sciences Center, in a manner illustrated in Figure 2. A tungsten lamp was put at the focal point of an off-axis parabolic mirror. The emerging planar wavefront thereafter illuminated the reference panel at a known angle. The radiance reflected in a direction normal to the surface was then measured using a radiometer built by Che. Thereafter the reference panel was removed, and a primary standard surface put in its place. This primary standard was a Halon panel which had been calibrated by NBS on February 8, 1984. (They determined the reflectance factor $R_{NBS}(45°/0°)$ for this surface.)

In the first phase of the field panel calibration, the reflectance factor $R_{ref}(45°/0°)$ was determined. This was computed from the following

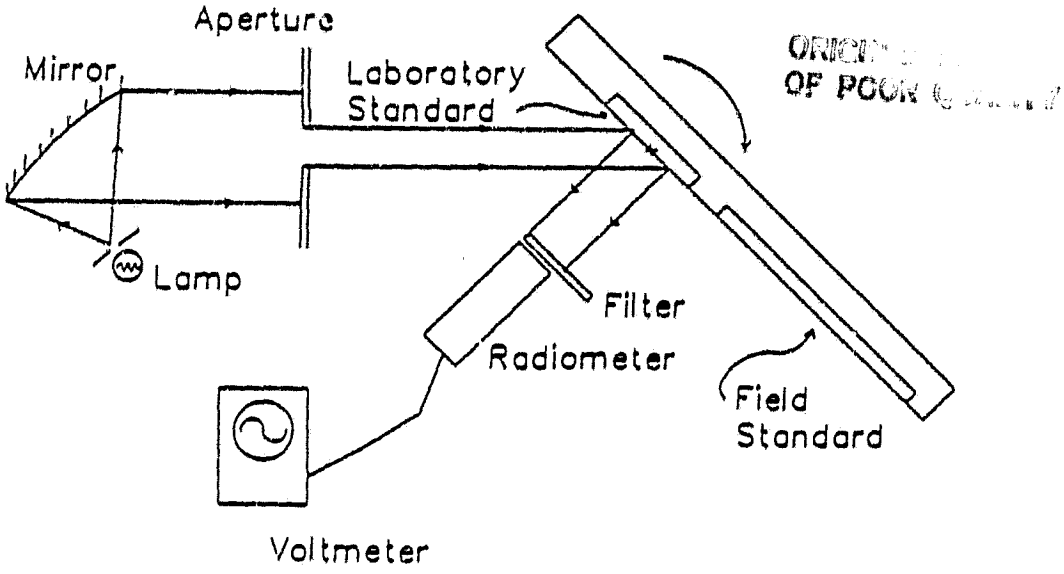

Figure 2. Laboratory set-up for the calibration of field reflectance panels.

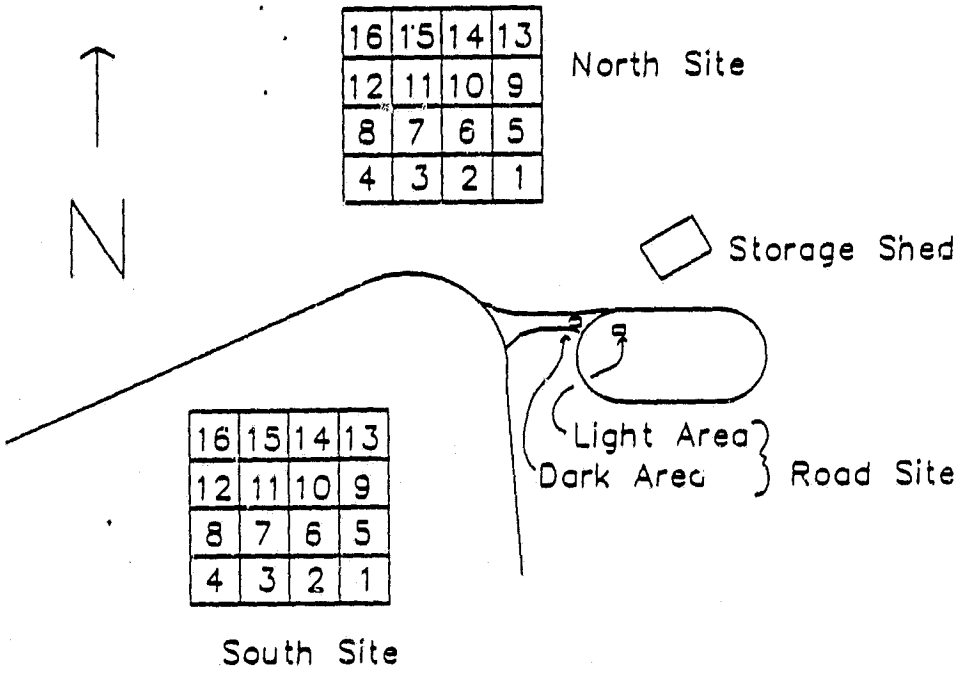

Figure 3. Schematic of Chuck Site test area.

Table 3. Laboratory calibration of $BaSO_4$ panel.

THE REFLECTANCE FACTOR OF $BaSO_4$ PANEL NO.5

Irradiance Angle(deg.)	430-470nm	530-570nm	630-670nm	830-870nm
10	1.0420	1.0355	1.0205	0.9858
15	1.0196	1.0138	0.9990	0.9651
20	1.0011	0.9945	0.9807	0.9479
25	0.9836	0.9779	0.9642	0.9331
30	0.9668	0.9610	0.9479	0.9185
35	0.9499	0.9449	0.9327	0.9045
40	0.9326	0.9279	0.9169	0.8905
45	0.9155	0.9119	0.9007	0.8773
50	0.8971	0.8937	0.8851	0.8627
55	0.8783	0.8765	0.8676	0.8474
60	0.8597	0.8582	0.8498	0.8326
65	0.8380	0.8390	0.8310	0.8157
70	0.8157	0.8174	0.8127	0.7986
75	0.7926	0.7929	0.7892	0.7789

Data: July 12,1984

Sample: $BaSO_4$ Panel No.5

Reference: Halon calibrated at (45/0) geometry by NBS (Feb. 8,1984)

Location: Infra. Lab.,OSC

Viewing Zenith Angle: 0 deg.

Irradiance Angle: 10-75 deg.

Table 4. Laboratory calibration of Halon panel.

THE REFLECTANCE FACTOR OF HALON PANEL (RAY'S)

Irradiance Angle(deg)	430-470nm	530-570nm	630-670nm	830-870nm
10	0.9965	1.0007	1.0020	1.0042
15	0.9892	0.9949	0.9951	0.9973
20	0.9829	0.9872	0.9888	0.9901
25	0.9741	0.9794	0.9804	0.9816
30	0.9648	0.9702	0.9716	0.9728
35	0.9556	0.9597	0.9618	0.9636
40	0.9442	0.9489	0.9499	0.9515
45	0.9319	0.9368	0.9377	0.9391
50	0.9166	0.9210	0.9231	0.9253
55	0.8991	0.9042	0.9061	0.9073
60	0.8784	0.8832	0.8860	0.8877
65	0.8539	0.8608	0.8633	0.8638
70	0.8221	0.8297	0.8323	0.8343
75	0.7805	0.7872	0.7919	0.7944

Data: July 12,1984

Sample: Halon panel (Ray's)

Reference: Halon calibrated at (45/0) geometry by NBS (Feb.8, 1984)

Location: Infra. Lab.,OSC

Viewing Zenith Angle: 0 deg.

Irradiance angle: 10-75 deg.

$$R_{ref}(45°/0°) = \frac{V_{ref}(45°/0°) * R_{NBS}(45°/0°)}{V_{NBS}(45°/0°)} \quad (2)$$

Next, the desired reflectance factor was computed from

$$R_{ref}(\theta/0°) = \frac{V_{ref}(\theta/0°) * \cos 45° * R_{ref}(45°/0°)}{V_{ref}(45°/0°) * \cos\theta} \quad (3)$$

The above steps were repeated for four spectral bandpass filters, each 40 nm wide. The measurement uncertainty was estimated to be less than 1%. A small error in the reflectance factor was also introduced due to the non-uniformity of the panels. In the field the radiance reflected from the panels was averaged over a larger area. This was due to the 15° FOV, as compared to the 1° FOV of the laboratory radiometer. The results of the panel calibration are shown in Table 3 for the $BaSO_4$ panel, and in Table 4 for Ray Jackson's Halon panel.

Reflectance Data

Both the Barnes data and the panel calibration data were used to determine the reflectance factors of each of the test sites at White Sands. It is noted that the field measurements were taken at several times throughout the morning. Those data taken closest to the time of the Landsat overpass, 11:07:40 MDT, were used in the radiance computations.

Several interpolations had to be made on the laboratory calibration data. The solar zenith angles were first computed for those times at which a field measurement of the sands was taken. The panel reflectance factors of Tables 3 and 4 were next interpolated to find the corresponding reflectance factors at these angles, for the four spectral filters available on Che's radiometer. These wavelengths differ from

those of the Barnes, therefore one more interpolation was necessary. The intermediate computations were used to compute the reflectances for the eight Barnes' wavelengths. (The Barnes' wavelengths correspond to those of the TM, for bands 1-4.)

The reflectance factors of the gypsum are determined from the above computed panel reflectances via Equation (1) above. A summary of this data reduction is given in Table 5. Only the data in channels 1-4 are used here. Reflectance factors are given for pixels 1-16. A schematic of the site, which identifies these pixels is shown in Figure 3.

Radiative Transfer Computations

The mean reflectance values, given in the bold type of Table 5, were used as input to the radiative transfer code. Also input were the atmospheric components listed in Table 2. The usual model assumptions were made for the aerosols. The maximum, minimum, and incremental radial sizes were 5.02, 0.02, and 0.04 μm, respectively. A refractive index of 1.54-0.01i was assumed. The code was run for both a solar zenith angle of 25° and 35°. The output, given in Table 6, is normalized for an exo-atmospheric solar irradiance of 1. After interpolating the data for a solar angle of 29.22° (that corresponding to the time of the overpass) the output is multiplied by the appropiate irradiance value. These final values are given in Table 7. They are the radiances that were incident on the TM sensor, for the morning of July 8.

Summary

Because of instrumentation problems and difficulties in accurately mapping ground reflectance due to the helicopter photography not being

Table 5. Absolute Reflectance of White Sands test sites.

North Site

TIME	ABSOLUTE REFLECTANCE CH(1) . . . CH(7)						
BaSO4							
10:52	.957	.952	.939	.915	.858	.839	.715
11:02	.964	.959	.946	.921	.863	.844	.718
ROAD							
10:54	.510	.577	.619	.650	.625	.527	.259
PIXELS 1-4,8							
10:57	.503	.573	.616	.648	.620	.517	.246
10:57	.510	.581	.627	.660	.632	.527	.236
10:58	.515	.584	.629	.661	.631	.525	.244
10:59	.530	.601	.645	.680	.646	.535	.231
11:01	.504	.571	.617	.652	.629	.526	.231
BASO4							
11:02	.964	.959	.946	.921	.863	.844	.718
11:08	.968	.963	.950	.924	.866	.846	.719
PIXELS 7-5							
11:04	.475	.538	.579	.610	.589	.492	.233
11:05	.488	.552	.594	.626	.601	.497	.230
11:06	.504	.571	.613	.643	.611	.502	.224
BASO4							
11:08	.968	.963	.950	.924	.866	.846	.719
11:15	.973	.968	.954	.929	.869	.849	.719
PIXELS 9-12							
11:08	.488	.555	.599	.630	.605	.501	.230
11:10	.504	.574	.620	.653	.623	.511	.229
11:11	.512	.580	.624	.657	.627	.519	.228
11:12	.526	.597	.643	.676	.637	.520	.213
BASO4							
11.15	.973	.968	.954	.929	.869	.849	.719
11.20	.976	.971	.958	.932	.871	.851	.720
PIXELS 13-16							
11.17	.501	.566	.608	.637	.611	.512	.252
11.18	.533	.602	.644	.674	.640	.533	.225
11.19	.511	.581	.624	.656	.631	.526	.228
11.20	.513	.583	.626	.656	.621	.508	.215
CUMULATIVE:							
MEAN	.507	.576	.619	.651	.622	.516	.231
SDEV	.015	.017	.018	.019	.015	.013	. .

Table 5. Continued

South Site

ABSOLUTE REFLECTANCE

TIME	CH(1)	. . .	CH(7)				
Halon							
10:58	.965	.968	.970	.971	.973	.974	.980
11:09	.969	.973	.974	.975	.977	.978	.983
1ST SCAN (PIXELS 1-16)							
10:59	.489	.551	.599	.642	.625	.500	.233
10:59	.494	.557	.601	.638	.618	.497	.241
11:00	.491	.548	.590	.627	.604	.481	.229
11:00	.468	.529	.573	.612	.591	.468	.229
11:01	.487	.546	.588	.626	.600	.480	.246
11:01	.493	.550	.592	.632	.606	.482	.228
11:02	.509	.572	.615	.653	.630	.508	.251
11:02	.514	.576	.618	.658	.628	.500	.231
11:03	.486	.546	.590	.629	.614	.491	.236
11:04	.503	.567	.611	.650	.634	.519	.256
11:04	.516	.578	.622	.660	.637	.512	.243
11:05	.498	.559	.603	.641	.621	.500	.241
11:05	.510	.572	.616	.654	.624	.492	.228
11:06	.510	.569	.610	.647	.616	.489	.230
11:06	.506	.567	.610	.650	.632	.514	.250
11:07	.503	.561	.603	.643	.622	.500	.250
MEAN	.499	.559	.603	.641	.619	.496	.239
SDEV	.013	.014	.013	.013	.013	.014	.010
Halon							
11:16	.972	.975	.976	.977	.980	.980	.986
11:27	.976	.979	.980	.981	.984	.984	.989
2ND SCAN (PIXELS 1-16)							
11:16	.492	.552	.594	.634	.619	.499	.247
11:17	.495	.561	.607	.646	.625	.500	.240
11:17	.494	.557	.601	.638	.616	.488	.236
11:18	.493	.555	.601	.640	.621	.494	.239
11:18	.499	.558	.600	.638	.612	.487	.248
11:19	.512	.573	.618	.659	.633	.503	.235
11:19	.508	.571	.614	.653	.629	.502	.238
11:20	.520	.582	.626	.666	.638	.503	.234
11:21	.501	.563	.610	.651	.633	.505	.242
11:21	.521	.587	.633	.673	.654	.527	.250
11:22	.519	.582	.626	.665	.643	.513	.239
11:22	.518	.579	.623	.662	.642	.517	.249
11:23	.520	.584	.630	.670	.639	.500	.229
11:24	.513	.573	.618	.659	.633	.502	.244
11:24	.507	.573	.618	.658	.640	.520	.254
11:25	.514	.574	.616	.655	.630	.501	.250
MEAN	.508	.570	.615	.654	.632	.504	.242
SDEV	.011	.011	.012	.012	.011	.011	.007

Table 5. Continued

Road Site

TIME	ABSOLUTE REFLECTANCE CH(1)						CH(7)
BASO4							
10:27	.940	.935	.924	.900	.846	.828	.711
10:32	.943	.939	.927	.903	.849	.831	.711
1ST DARK AREA							
10:28	.445	.495	.529	.553	.540	.472	.235
10:28	.459	.508	.541	.562	.543	.473	.228
10:28	.463	.513	.544	.565	.543	.470	.223
10:29	.458	.509	.543	.564	.543	.470	.224
10:29	.473	.525	.559	.581	.558	.481	.226
MEAN	.459	.510	.543	.565	.545	.473	.227
SDEV	.010	.011	.011	.010	.007	.005	.005
1ST LIGHT AREA							
10:29	.516	.580	.623	.656	.607	.480	.178
10:30	.501	.560	.600	.632	.585	.463	.169
10:30	.504	.564	.602	.635	.589	.469	.174
MEAN	.507	.568	.608	.641	.594	.471	.174
SDEV	.008	.010	.013	.013	.012	.009	.004
BASO4							
10:37	.947	.942	.930	.906	.851	.832	.712
10:40	.949	.944	.932	.908	.852	.834	.712
2ND DARK AREA							
10:37	.447	.495	.527	.549	.534	.467	.233
10:38	.455	.505	.538	.559	.543	.473	.233
10:38	.457	.506	.538	.560	.541	.469	.224
10:38	.457	.507	.540	.562	.541	.467	.224
10:38	.476	.525	.558	.579	.556	.476	.223
MEAN	.458	.508	.540	.562	.543	.470	.227
SDEV	.011	.011	.011	.011	.008	.004	.005
2ND LIGHT AREA							
10:39	.516	.578	.618	.651	.604	.477	.177
10:39	.505	.566	.605	.638	.590	.463	.167
10:40	.504	.561	.597	.628	.583	.464	.172
MEAN	.509	.568	.607	.639	.592	.468	.172
SDEV	.007	.009	.011	.011	.010	.008	.005
BASO4							
11:38	.989	.983	.969	.942	.879	.859	.722
11:42	.991	.986	.972	.945	.881	.860	.723

Road Site. Continued

3RD DARK AREA							
11:39	.478	.534	.568	.589	.569	.495	.245
11:39	.479	.534	.569	.591	.567	.488	.233
11:40	.487	.543	.577	.598	.573	.493	.236
11:40	.485	.542	.577	.598	.571	.490	.233
11:40	.499	.554	.587	.608	.580	.495	.232
MEAN	.486	.541	.576	.597	.572	.492	.236
SDEV	.008	.008	.008	.008	.005	.003	.005
3RD LIGHT AREA							
11.41	.540	.608	.651	.682	.629	.498	.189
11.41	.530	.597	.639	.669	.614	.481	.176
11.42	.530	.598	.639	.667	.613	.485	.181
MEAN	.533	.601	.643	.673	.619	.488	.182
SDEV	.006	.006	.007	.008	.009	.009	.006

Table 6. Herman Code Output

WAV	τMie	τRay	τoz	θz	ρ	Edir	Edif	Lpath	Lt
0.486	0.0864	0.1421	0.0055	25	0.507	0.7001	0.1519	0.0246	0.1334
					0.499		0.1504	0.0244	0.1313
0.486	0.0864	0.1421	0.0055	35	0.507	0.6156	0.1417	0.0223	0.1190
					0.499		0.1404	0.0222	0.1172
0.571	0.0777	0.0735	0.0232	25	0.576	0.7477	0.1113	0.0134	0.1457
					0.559		0.1088	0.0133	0.1413
0.571	0.0777	0.0735	0.0232	35	0.576	0.6621	0.1028	0.0121	0.1299
					0.559		0.1006	0.0120	0.1260
0.661	0.0706	0.0406	0.0114	25	0.619	0.7916	0.9078	0.0080	0.1618
					0.603		0.8880	0.0079	0.1574
0.661	0.0706	0.0406	0.0114	35	0.619	0.7053	0.8337	0.0072	0.1447
					0.603		0.8160	0.0071	0.1407
0.838	0.0605	0.0156	0.0013	25	0.651	0.8321	0.6780	0.0033	0.1759
					0.641		0.6683	0.0032	0.1730
0.838	0.0605	0.0156	0.0013	35	0.651	0.7453	0.6182	0.0030	0.1578
					0.641		0.6095	0.0029	0.1552

where

E_{dir} The downward direct solar irradiance at the ground, $\cos\theta_z * \exp(-\tau_{ext} \sec\theta_z)$.

E_{dif} The downward diffuse solar irradiance at the ground.

L_{path} The upward path radiance at the TM, $L_T-(E_{dir}+E_{dif}) * \exp(-\tau_{ext} \sec 5^\circ)\rho/\pi$

L_t The total radiance at the TM at a 5° nadir angle.

Note all irradiance and radiance values are normalized for an exo-atmospheric solar irradiance of 1.

Table 7. Computed radiance at Landsat sensors.

L ($mW/cm^2sr\ \mu m$)

Band	North Site	South Site
1	23.18	22.82
2	25.13	24.37
3	23.82	23.17
4	17.64	17.35

vertical, the results of the July 8, 1984 measurement will have high uncertainties associated with them. However, the measurement attempt was worthwhile because of the experience gained in instrument operation and measurement.

There are still a few remaining computations to be made with the July 8th data. Only a few discrete points of data were taken at the pixel centers of the two test sites. We are currently exploring the usage of the aerial photography (the slide imagery which has been scanned) to better characterize the reflectance of the area. The radiosonde and humidity data will also be looked at. Once the optical depth component τ_{H2O} can be determined, the Herman code will be rerun to account for atmospheric water vapor in band 4. The diffuse to direct data will be compared with the Herman code output. Finally, it remains to inspect the Landsat imagery, identify our test site, and compute incident radiance, as determined from the pre-flight data. A comparison can then be made of our in-flight calibration, to that made based upon pre-flight data and the internal calibrator data. The calibrations of bands 5 and 7 will not be investigated for this date. No atmospheric data are available at these wavelengths and the optical depth components cannot be computed. The Castle spectropolarimeters will be equipped with a filter set which will allow us, in the future, to do calibrations in the short wave infrared.

References

1. Neckel, H. and D. Labs. "Improved data of solar spectral irradiance from 0.33 to 1.25 μm". Solar Physics, Vol. 74, p. 231, 1981.

2. Palmer, James M. "Effective bandwidths for Landsat-4 and Landsat-4' multispectral scanner and thematic mapper subsystems". IEEE trans, Geoscience and Remote Sensing, Vol. GE-22, p.336-338, 1984.

APPENDIX A

Reflectance

The nomenclature, measuring geometry, and techniques associated with determining the reflectance of a given surface are quite varied. With this in mind, the technical basis of our measurements at White Sands is presented here. We are interested in the directional properties, as well as the magnitude, of the reflectance at the field site, for this reason we determine the reflectance factor. Reflectance factor and other quantities are defined below. A spectral dependance is assumed for each quantity. All of our reflectance measurements are made with finite spectral bandwidths. These are, in general, the 40 nm bandwidths of a laboratory radiometer, or those bandwidths associated with the Thematic Mapper and the Barnes modular multiband radiometer.

Definitions and Nomenclature

Reflectance Factor, $R(\theta,\phi;\theta',\phi')$ (unitless). Ratio of the flux reflected by a sample surface to that which would be reflected into the same beam geometry by a lossless, lambertian surface which is identically irradiated. Thus,

$$R(\theta,\phi;\theta',\phi') = \frac{\int_{IFOV} L_t(\theta',\phi')\cos\theta' \sin\theta' \, d\theta' \, d\phi'}{\int_{IFOV} L_p(\theta',\phi')\cos\theta' \sin\theta' \, d\theta' \, d\phi'} \qquad (1)$$

is the reflectance factor measured with a detector having a given

instantaneous field of view (IFOV). L_t is the radiance reflected off the sample target, and L_p is the radiance reflected off a perfect (lossless), diffuse surface. The incident beam originates from (θ,ϕ), and the reflected beam is viewed in the direction (θ',ϕ').

Reflectance ρ (unitless). Ratio of the reflected flux to the incident flux. When referring to this parameter one needs to specify if the flux is integrated over the reflecting hemisphere, or if the reflected flux is measured within a given cone angle. The hemispherical reflectance can be related to the reflectance factor by

$$\rho = \int_{2\pi}\int_{\pi/2} L_t(\theta',\phi')\cos\theta' \sin\theta' \, d\theta' \, d\phi'/E \qquad (2)$$

$$= R(\theta,\phi;2\pi)$$

where E is the incident irradiance, generally from a well collimated beam. It is computed from

$$E = \int \int_{\omega} L_t(\theta,\phi)\cos\theta \sin\theta \, d\theta \, d\phi \qquad (3)$$

Note the integration is over the solid angle $d\omega=\sin\theta \, d\theta \, d\phi$.

Bidirectional Reflectance Distribution Function (BRDF), f (sr^{-1}). The ratio of the radiance reflected in the direction (θ',ϕ') to the total irradiance on the surface from the direction (θ,ϕ).

$$f(\theta,\phi;\theta',\phi') = L_t(\theta',\phi')/E \qquad (4)$$

The quantity $R(\theta,\phi;2\pi)$ is equivalent to ρ. The 2π denotes that the reflectance factor has been integrated over a hemisphere. $R(\theta;d)$, or $R(\theta/d)$, is an equivalent description, the "d" denoting that diffuse reflectance has been accounted for. Even when an integration is not

implied, the symbols ϕ and ϕ' are often dropped for simplicity (as is true for any of the above parameters).

Choice of the Reflectance Factor

In calibrating the TM we are interested in knowing the radiance reflected from the gypsum sands into a number of discrete angles. This allows both the directly and diffusely reflected solar radiation to be accurately characterized. Such a complete BRDF measurement is, however, both time consuming and difficult to measure. The equipment required is relatively complex, and there are difficulties associated with measuring the incident irradiance. Instead we have chosen to characterize the gypsum by the reflectance factor $R(\theta_z;0°)$. This accurately describes the flux that is directly reflected towards the Landsat sensors. As the gypsum sands are not truely lambertian, some error is incured in not computing the full BRDF. Without the BRDF data, a lambertian surface is assumed. Thus an overestimate is made in the radiance not directly reflected towards the TM. Due to atmospheric multiple scattering in the atmosphere, some of this flux edventually reaches the sensors. This is the diffuse component of the radiance. The error made in predicting this term increases with increased multiple scattering, and with departure from a lambertian behavior. Even so, the usage of the reflectance factor is justified. This is because the radiance received at the TM is dominated by the direct component, and multiple scattering is minimal for clear atmospheric conditions.

Calibrating the Field Reference

The reflectance factor is measured with respect to a reference panel which is calibrated in the laboratory to account for its non-ideal characteristics. The calibration procedure was briefly described in the body of the report. Here a development of the equations used in the two step calibration procedure is given.

To begin with, it is assumed that a laboratory standard is available. In our case a 50 mm diameter Halon disc was used which had been calibrated by NBS to determine $R_{NBS}(45°;0°)$. The fictional parameter $V_p(45°;0°)$ is thereby computed:

$$V_p(45°;0°) = \frac{V_{NBS}(45°;0°)}{R_{NBS}(45°;0°)} \tag{5}$$

This is the voltage that would have been measured had a perfect (lossless) lambertian surface been present.

Using the above, the reflectance factor of the reference panel is found for the same geometry:

$$R_{ref}(45°;0°) = \frac{V_{ref}(45°;0°)}{V_p(45°;0°)} \tag{6}$$

$$= \frac{V_{ref}(45°;0°) * R_{NBS}(45°;0°)}{V_{NBS}(45°;0°)}$$

In the next phase of calibration, the reflectance factor measurements are made at the angle of interest, θ. For the ideal lambertian surface the detector response at angle θ is easily predicted from the response at 45°. Such a surface reflects radiance uniformly into the upper hemisphere, thereby reflecting a factor of $1/\pi$ of the incident irradiance. Thus, for this perfect (ρ=1) lambertian surface, illuminated with a beam of irradiance $E(\theta)$, the following relationships

hold:

$$V_p(45°;0°) = R * E(45°)\ \rho/\pi = R * E_\theta\ \cos45°/\pi \tag{7}$$

$$V_p(\theta;0°) = R * E(\theta)\ \rho/\pi = R * E_\theta\ \cos\theta/\pi \tag{8}$$

$$= \frac{V_p(45°;0°) * \cos\theta}{\cos45°}$$

The detector is assumed to have a given response, R, to the incoming radiance. This latter result is now substituted into the equation for $R_{ref}(\theta;0°)$, to yield the final, desired result:

$$R_{ref}(\theta;0°) = \frac{V_{ref}(\theta;0°)}{V_p(\theta;0°)} \tag{9}$$

$$= \frac{V_{ref}(\theta;0°) * \cos45°}{V_p(45°;0°) * \cos\theta}$$

$$= \frac{V_{ref}(\theta;0°) * \cos45° * R_{ref}(45°;0°)}{V_{ref}(45°;0°) * \cos\theta}$$

APPENDIX B

Radiosonde and atmospheric data for July 8th, as provided by the Atmospheric Sciences Laboratory, White Sands Missle Range.

PROJECT SURFACE OBSERVATION

MISSION CODE LANDSAT 5 STATION CHUCK SITE

DATE 08 (DAY) 07 (MONTH) 84 (YEAR) X= 32° 54' Y= 106° 18' H= 3912.75ft

TIME M D J	PRESSURE mbs	TEMPERATURE °F	TEMPERATURE °C	DEW POINT °F	DEW POINT °C	RELATIVE HUMIDITY %	DENSITY gm/m³	WIND DIRECTION degs Tn	WIND SPEED kts	WIND CHARACTER kts	VISIBILITY
0730	883.8	68.4	20.2	54.3	12.4	61	1042	105	01		40
0930	883.4	81.0	27.2	56.1	13.4	42	1019	095	01		40
0945	883.4	83.3	28.5	55.2	12.9	38	1015	100	01		40

OBSTRUCTIONS TO VISIBILITY	CLOUDS 1st LAYER AMT	1st LAYER TYPE	1st LAYER HGT	2nd LAYER AMT	2nd LAYER TYPE	2nd LAYER HGT	3rd LAYER AMT	3rd LAYER TYPE	3rd LAYER HGT	REMARKS
							1	Ci	25000	
							2	Ci	25000	
							2	Ci	25000	

PSYCHROMETRIC COMPUTATION

TIME:	0730	0930	0945
DRY BULB TEMP.	20.2	27.2	28.5
WET BULB TEMP.	15.2	18.0	18.1
WET BULB DEPR.	5.0	9.2	10.4
DEW POINT	12.4	13.4	12.9
RELATIVE HUMID.	61	42	38

R Savage
OBSERVER

VERIFIER

ORIGINAL PAGE IS OF POOR QUALITY

DELAS-MS-MT-WS FORM 12
01 NOV 1980

Supersedes AMSEL-BL-MT-WS Form 12, 28 Aug 72 and all project surface observation forms, except DIVAD Surface Observation for.

PROJECT SURFACE OBSERVATION

MISSION CODE LANDSAT-5 STATION CHUCK SITE

DATE 08 (DAY) 07 (MONTH) 84 (YEAR) X= 32°54' Y= 106°18' H= 3912.75ft

TIME M D L	PRESSURE mbs	TEMPERATURE °F	TEMPERATURE °C	DEW POINT °F	DEW POINT °C	RELATIVE HUMIDITY %	DENSITY gm/m³	WIND DIRECTION degs Tn	WIND SPEED kts	WIND CHARACTER kts	VISIBILITY
1000	883.3	84.4	29.1	55.2	12.9	37	1012	090	02		40
1015	883.2	86.0	30.0	59.0	15.0	40	1009	095	03		40
1030	883.2	86.4	30.2	59.2	15.1	40	1008	080	05		40

OBSTRUCTIONS TO VISIBILITY	CLOUDS 1st LAYER AMT	1st LAYER TYPE	1st LAYER HGT	2nd LAYER AMT	2nd LAYER TYPE	2nd LAYER HGT	3rd LAYER AMT	3rd LAYER TYPE	3rd LAYER HGT	REMARKS
	1	Cu	6000	0	AC	12000	2	Ci	25000	
	1	Cu	6000	0	AC	12000	2	Ci	25000	
	2	Cu	6000	0	AC	12000	2	Ci	25000	

PSYCHROMETRIC COMPUTATION

TIME:	1000	1015	1030
DRY BULB TEMP.	29.1	30.0	30.2
WET BULB TEMP.	18.3	19.7	19.8
WET BULB DEPR.	10.8	10.3	10.4
DEW POINT	12.9	15.0	15.1
RELATIVE HUMID.	37	40	40

R Savage
OBSERVER

VERIFIER

DELAS-MS-MT-WS FORM 12
01 NOV 1980

Supersedes ANSEL-BL-MT-MS Form 12, 28 Aug 72 and all project surface observation forms, except DIVAD Surface Observation for.

PROJECT SURFACE OBSERVATION

MISSION CODE LANDSAT-5 STATION CHUCK SITE

DATE 08 (DAY) 07 (MONTH) 84 (YEAR) X= 32°54' Y= 106°18' H= 3912.75ft

TIME M D T	PRESSURE mbs	TEMPERATURE °F	TEMPERATURE °C	DEW POINT °F	DEW POINT °C	RELATIVE HUMIDITY %	DENSITY gm/m³	WIND DIRECTION degs Tn	WIND SPEED kts	WIND CHARACTER kts	VISIBILITY
1045	883.2	86.9	30.5	58.8	14.9	39	1007	095	04		40
1100	883.1	88.3	31.3	58.5	14.7	36	1005	095	04		40
1107	883.0	90.0	32.2	57.9	14.4	34	1002	100	04		40

OBSTRUCTIONS TO VISIBILITY	CLOUDS 1st LAYER AMT	1st LAYER TYPE	1st LAYER HGT	2nd LAYER AMT	2nd LAYER TYPE	2nd LAYER HGT	3rd LAYER AMT	3rd LAYER TYPE	3rd LAYER HGT	REMARKS
	2	Cu	6000	0	AC	12000	2	Ci	25000	
	2	Cu	6000	0	AC	12000	2	Ci	25000	
	2	Cu	6000	0	AC	12000	2	Ci	25000	

PSYCHROMETRIC COMPUTATION

TIME:	1045	1100	1107
DRY BULB TEMP.	30.5	31.3	32.2
WET BULB TEMP.	19.8	19.9	20.0
WET BULB DEPR.	10.7	11.4	12.2
DEW POINT	14.9	14.7	14.4
RELATIVE HUMID.	39	36	34

R. Savage
OBSERVER

VERIFIER

DELAS-MS-MT-WS FORM 12
01 NOV 1980

Supersedes AMSEL-BL-MT-WS Form 12, 28 Aug 72 and all project surface observation forms, except DIVAD Surface Observation for.

PROJECT SURFACE OBSERVATION

MISSION CODE LANDSAT-5 STATION CHUCK SITE

DATE 08 (DAY) 07 (MONTH) 84 (YEAR)

X= 32°54' Y= 106°18' H= 3912.75ft

TIME MDT	PRESSURE mbs	TEMPERATURE °F	TEMPERATURE °C	DEW POINT °F	DEW POINT °C	RELATIVE HUMIDITY %	DENSITY gm/m³	WIND DIRECTION degs Tn	WIND SPEED kts	WIND CHARACTER kts	VISIBILITY
1115	882.9	92.1	33.4	57.6	14.2	31	998	100	03		40
1130	882.8	95.0	35.0	57.0	13.9	28.	993	095	04		40

OBSTRUCTIONS TO VISIBILITY	CLOUDS 1st LAYER AMT	1st LAYER TYPE	1st LAYER HGT	2nd LAYER AMT	2nd LAYER TYPE	2nd LAYER HGT	3rd LAYER AMT	3rd LAYER TYPE	3rd LAYER HGT	REMARKS
	2	Cu	6000	0	AC	12000	2	Ci	25000	
	2	Cu	6000	0	AC	12000	2	Ci	25000	

PSYCHROMETRIC COMPUTATION

TIME:	1115	1130	
DRY BULB TEMP.	33.4	35.0	
WET BULB TEMP.	20.2	20.5	
WET BULB DEPR.	13.2	14.5	
DEW POINT	14.2	13.9	
RELATIVE HUMID.	31	28	

ORIGINAL PAGE IS OF POOR QUALITY

P. Savage
OBSERVER

VERIFIER

DELAS-MS-MT-WS FORM 12
01 NOV 1980

Supersedes ANSEL-GL-MT-WS Form 12, 28 Aug 72 and all project surface observation forms, except DIVAD Surface Observation for.

STAT. ALTITUDE 3989.0 FEET MSL   SIGNIFICANT LEVEL DATA   GEODETIC COORDINATES

JULY 54   0600 HRS MST   1900370365   32.43063 LAT DEG

ASCENSION NO. 355   WHITE SANDS   106.37033 LON DEG

PRESSURE MILLIBARS	GEOMETRIC ALTITUDE MSL FEET	TEMPERATURE AIR DEGREES CENTIGRADE	TEMPERATURE DEWPOINT DEGREES CENTIGRADE	REL.HUM. PERCENT
881.0	3990.0	25.0	12.2	40.0
871.1	4215.5	24.3	3.7	37.0
850.0	5018.7	22.7	9.1	42.0
795.1	6318.2	20.0	7.4	44.0
747.1	8671.9	15.8	5.1	49.0
725.5	9438.5	14.0	2.9	47.0
700.0	10475.9	11.5	2.5	54.0
681.9	11174.7	9.3	1.9	50.0
651.0	12415.9	6.7	-.4	52.0
634.0	13154.3	4.0	-1.6	57.0
615.4	13916.2	3.2	-10.4	36.0
607.7	14294.9	3.0	-14.5	25.0
564.0	15351.0	1.5	-15.0	23.0
558.3	16579.4	.1	-20.7	19.0
516.7	18551.4	-4.5	-24.6	19.0
500.0	19497.9	-7.1	-26.7	19.0
475.8	20625.7	-7.3	-23.1	17.0
400.0	25044.5	-17.0	-34.1	21.0
343.5	26744.0	-24.4	-40.8	20.0
300.0	31941.0	-33.3	-43.0	21.0
269.2	37510.5	-36.4	-50.7	21.0
264.0	34850.5	-39.7	-52.6	24.0
250.0	36576.9	-42.9		
223.3	38554.4	-49.1		
200.0	40911.8	-53.9		
170.2	44073.9	-60.7		
150.0	46845.7	-64.0		
133.7	49078.5	-67.8		
119.2	51413.1	-70.3		
100.0	54848.5	-71.2		
85.0	58072.5	-63.8		
70.0	62031.1	-54.7		
58.4	65835.4	-51.3		
50.0	68925.5	-55.7		
44.4	71290.3	-58.1		
35.0	75844.4	-52.9		
30.0	79591.3	-53.4		
24.0	84441.6	-51.7		
20.0	88425.3	-46.1		
15.6	92559.9	-42.5		

ORIGINAL PAGE IS
OF POOR QUALITY

STATION ALTITUDE 3759.0 FEET MSL
6 JULY 84 0600 HRS MST
ASCENSION NO. 356

SIGNIFICANT LEVEL DATA
1980373366
WHITE SANDS

GEODETIC COORDINATES
32.43043 LAT DEG
106.33033 LON DEG

PRESSURE MILLIBARS	GEOMETRIC ALTITUDE MSL FEET	TEMPERATURE AIR DEGREES CENTIGRADE	DEW POINT	REL.HUM. PERCENT
12.4	97191.1	-40.1		

STATION ALTITUDE 3999.0 FEET MSL
6 JULY 84 0830 HRS MST
ASCENSION NO. 366

UPPER AIR DATA
19800206
WHITE SANDS

GEODETIC COORDINATES
32.40043 LAT DEG
106.37033 LON DEG

GEOMETRIC ALTITUDE MSL FEET	PRESSURE MILLIBARS	TEMPERATURE AIR DEGREES	TEMPERATURE DEWPOINT CENTIGRADE	REL.HUM. PERCENT	DENSITY GM/CUBIC METER	SPEED OF SOUND KNOTS	WIND DATA DIRECTION DEGREES(TN)	WIND DATA SPEED KNOTS	INDEX OF REFRACTION
3999.0	991.0	20.9	1.2	41.0	1017.5	675.9	.0	.0	1.000295
4000.0	990.7	20.8	12.0	79.9	1016.5	676.8	190.0	.1	1.000285
4500.0	955.5	23.9	6.6	38.3	1010.1	673.1	190.7	2.5	1.000274
5000.0	953.6	22.7	9.1	41.9	996.2	671.9	190.9	5.9	1.000272
5500.0	935.[illegible]	22.0	8.7	42.5	981.4	671.0	190.9	10.4	1.000268
6000.0	921.2	21.3	[illegible]	43.0	966.7	670.2	191.[illegible]	11.7	1.000263
6500.0	906.9	20.6	7.8	43.6	952.[illegible]	669.4	192.4	11.6	1.000259
7000.0	892.[illegible]	19.3	7.3	44.2	938.2	668.4	196.[illegible]	9.6	1.000254
7500.0	878.9	18.0	6.7	45.7	925.5	667.0	201.[illegible]	7.5	1.000250
8000.0	865.2	17.4	6.0	47.1	911.1	665.6	204.5	7.4	1.000246
8500.0	851.7	16.2	5.4	48.5	900.9	664.2	206.5	7.1	1.000241
9000.0	838.3	15.1	4.2	48.2	888.5	662.8	206.1	6.6	1.000236
9500.0	825.2	14.0	2.9	47.1	877.4	661.4	195.6	4.9	1.000233
10000.0	811.[illegible]	12.7	2.7	50.6	864.5	660.0	165.2	3.4	1.000227
10500.0	799.4	11.4	2.5	54.2	857.8	658.5	125.4	4.9	1.000224
11000.0	786.8	9.9	2.1	58.4	841.9	656.7	105.4	7.2	1.000221
11500.0	774.3	8.6	1.4	60.5	830.7	655.1	94.5	8.9	1.000217
12000.0	762.0	7.3	.4	61.3	819.3	653.6	89.1	10.7	1.000213
12500.0	749.9	6.0	-.6	62.6	808.1	652.1	84.1	12.3	1.000209
13000.0	737.9	4.5	-1.3	65.9	797.7	650.2	85.3	13.6	1.000205
13500.0	726.1	3.6	-5.0	57.2	786.0	649.0	88.3	14.8	1.000196
14000.0	714.5	3.2	-11.2	33.8	773.5	648.1	91.1	14.2	1.000185
14500.0	703.0	2.7	-14.7	26.4	760.5	647.4	98.7	13.5	1.000179
15000.0	691.6	2.0	-14.2	27.3	748.3	646.6	108.4	13.2	1.000175
15500.0	680.7	1.3	-15.5	26.9	736.2	645.5	118.4	13.5	1.000173
16000.0	669.[illegible]	.7	-17.9	23.1	724.1	645.3	127.2	14.9	1.000169
16500.0	658.1	.1	-20.5	19.3	712.1	644.3	133.4	16.0	1.000165
17000.0	646.5	-.9	-21.5	19.0	701.5	643.0	138.0	15.9	1.000162
17500.0	635.1	-2.1	-22.6	19.0	691.1	641.6	141.6	15.9	1.000159
18000.0	627.9	-3.2	-23.5	19.0	680.9	640.3	144.9	14.5	1.000155
18500.0	617.2	-4.4	-24.5	19.0	670.8	638.9	146.9	13.1	1.000154
19000.0	608.0	-5.6	-25.7	19.0	661.7	637.1	145.5	13.6	1.000151
19500.0	598.[illegible]	-7.1	-26.8	18.8	652.1	635.6	144.5	14.7	1.000149
20000.0	588.[illegible]	-7.[illegible]	-27.4	18.0	639.7	635.5	148.7	15.5	1.000146
20500.0	579.1	-7.5	-28.0	17.[illegible]	627.5	635.4	152.7	15.5	1.000143
21000.0	569.8	-9.1	-29.[illegible]	17.3	617.2	634.4	157.3	17.7	1.000141
21500.0	560.5	-9.[illegible]	-29.2	17.8	607.5	633.3	160.[illegible]	18.9	1.000[illegible]5
22000.0	551.[illegible]	-10.3	-29.9	18.2	599.1	631.7	162.4	19.6	1.000135
22500.0	542.[illegible]	-11.4	-30.[illegible]	18.7	589.8	630.4	162.[illegible]	19.5	1.000134
23000.0	533.[illegible]	-12.5	-31.[illegible]	19.1	579.7	629.1	161.9	18.4	1.000132

STATION ALTITUDE 3680.0 FEET MSL
1 JULY 84 0600 HRS MST
ASCENSION NO. 350

UPPER AIR DATA
19030306
WHITE SANDS

GEODETIC COORDINATES
32.43063 LAT DEG
106.37933 LON DEG

GEOPOTENTIAL ALTITUDE MSL FEET	PRESSURE MILLIBARS	TEMPERATURE AIR DEGREES CENTIGRADE	TEMPERATURE DEWPOINT CENTIGRADE	REL.HUM. PERCENT	DENSITY GM/CUBIC METER	SPEED OF SOUND KNOTS	WIND DATA DIRECTION DEGREES(TN)	WIND DATA SPEED KNOTS	INDEX OF REFRACTION
24500.0	476.3	-18.6	-31.4	19.6	570.7	627.7	159.0	17.4	1.000127
24600.0	471.0	-18.7	-32.6	21.1	561.9	626.4	154.9	17.0	1.000127
24700.0	465.8	-19.0	-33.3	20.5	553.1	625.1	152.5	15.2	1.000125
24800.0	460.7	-18.9	-34.2	21.0	544.5	623.7	150.4	15.4	1.000123
24900.0	455.6	-17.9	-34.4	20.9	535.7	622.5	150.0	14.1	1.000121
25000.0	450.6	-18.9	-35.8	20.7	526.3	621.3	149.6	13.2	1.000119
25100.0	445.6	-19.9	-36.7	20.6	518.2	620.0	149.1	12.2	1.000117
25200.0	440.7	-20.9	-37.6	20.5	509.7	618.8	148.9	13.7	1.000115
25300.0	435.8	-21.9	-38.5	20.3	501.3	617.6	148.9	13.4	1.000113
25400.0	430.9	-22.9	-39.5	20.2	493.1	616.3	148.3	11.5	1.000111
25500.0	426.1	-23.9	-40.4	20.1	485.0	615.1	147.3	9.2	1.000109
25600.0	421.3	-25.1	-41.4	20.1	477.3	613.8	142.5	7.7	1.000107
25700.0	416.7	-26.5	-42.5	20.2	469.9	611.9	136.1	5.3	1.000105
25800.0	412.0	-27.9	-43.6	20.4	462.7	610.1	127.9	4.9	1.000104
25900.0	407.5	-29.3	-44.8	20.5	455.5	608.4	115.5	3.8	1.000102
26000.0	403.0	-30.7	-45.9	20.7	448.5	606.7	96.5	2.9	1.000101
26100.0	398.5	-32.1	-47.3	20.9	441.7	604.9	92.6	3.7	1.000099
26200.0	394.1	-33.4	-48.1	21.0	434.3	603.2	91.1	4.9	1.000097
26300.0	389.8	-34.4	-49.0	21.0	427.2	602.0	82.3	5.2	1.000095
26400.0	385.5	-35.4	-49.8	21.0	419.7	600.7	75.9	7.6	1.000094
26500.0	381.2	-36.4	-50.7	21.0	412.4	599.5	69.1	9.9	1.000092
26600.0	376.9	-37.7	-51.3	22.1	405.5	597.8	64.9	9.7	1.000091
26700.0	372.8	-39.0	-52.1	22.2	399.0	596.2	62.1	9.5	1.000089
26800.0	368.6	-40.2	-53.9	21.3**	392.6	594.6	55.8	9.9	1.000088
26900.0	364.5	-41.5	-59.9	11.4**	386.3	593.0	43.8	8.0	1.000086
27000.0	360.5	-42.7	-74.5	1.6**	379.3	591.4	24.4	9.8	1.000084
27100.0	356.5	-44.0			372.9	589.8	9.5	11.5	1.000083
27200.0	352.7	-45.2			366.3	588.2	5.3	13.7	1.000082
27300.0	348.8	-46.5			360.1	586.6	3.7	15.6	1.000080
27400.0	345.1	-47.7			353.9	584.9	2.5	15.0	1.000079
27500.0	341.3	-49.0			347.8	583.3	1.1	16.5	1.000077
27600.0	337.7	-50.2			341.4	582.0	358.7	13.7	1.000076
27700.0	334.0	-51.0			335.1	580.6	357.1	20.6	1.000075
27800.0	330.4	-52.0			328.8	579.3	356.7	21.6	1.000073
27900.0	326.9	-53.1			322.7	578.0	356.9	20.2	1.000072
28000.0	323.4	-54.1			316.7	576.6	358.9	17.0	1.000071
28100.0	319.9	-55.1			310.6	575.3	3.4	13.8	1.000069
28200.0	316.5	-56.1			304.7	574.0	11.2	10.7	1.000068
28300.0	313.1	-57.1			299.3	572.6	7.8	9.6	1.000067
28400.0	309.8	-58.1			293.1	571.3	1.5	8.9	1.000065

** AT LEAST ONE ASSUMED RELATIVE HUMIDITY VALUE WAS USED IN THE INTERPOLATION.

UPPER AIR DATA
1800/03866
JUTTE SANDS

STATION ALTITUDE [illegible] FEET MSL
1 JULY 84 [illegible] HRS MST
ASCENSION NO. 356

GEODETIC COORDINATES
32.63043 LAT DEG
106.37033 LON DEG

GEOPOTENTIAL ALTITUDE MSL FEET	PRESSURE MILLIBARS	TEMPERATURE AIR DEGREES CENTIGRADE	TEMPERATURE DEWPOINT CENTIGRADE	REL.HUM. PERCENT	DENSITY GM/CUBIC METER	SPEED OF SOUND KNOTS	WIND DATA DIRECTION DEGREES(TN)	WIND DATA SPEED KNOTS	INDEX OF REFRACTION
43500.0	175.6	-59.1			257.5	559.9	346.9	8.6	1.000064
44000.0	172.[illegible]	-59.1			252.0	559.5	331.9	9.0	1.000063
44500.0	168.[illegible]	-61.5			276.4	557.4	324.7	10.9	1.000062
45000.0	164.[illegible]	-61.8			270.5	555.6	324.8	12.7	1.000060
45500.0	160.[illegible]	-62.3			264.7	555.7	342.2	13.9	1.000059
46000.0	156.4	-62.9			259.1	554.9	359.[illegible]	14.6	1.000058
46500.0	152.[illegible]	-63.6			253.5	554.0	17.5	14.9	1.000056
47000.0	148.8	-64.[illegible]			248.2	553.1	32.9	14.6	1.000055
47500.0	145.2	-65.1			243.0	552.0	45.8	14.2	1.000054
48000.0	141.[illegible]	-65.[illegible]			238.0	550.9	56.3	13.7	1.000053
48500.0	138.1	-66.7			233.0	549.8	67.4	13.6	1.000052
49000.0	134.7	-67.5			228.1	548.7	78.5	11.7	1.000051
49500.0	131.3	-68.1			223.2	547.8	81.0	9.8	1.000050
50000.0	128.1	-68.7			218.2	547.0	84.7	7.8	1.000049
50500.0	124.8	-69.3			213.3	546.3	92.0	6.3	1.000048
51000.0	121.7	-69.6			208.6	545.5	104.5	5.9	1.000046
51500.0	118.7	-70.3			203.8	544.8	112.9	7.8	1.000045
52000.0	115.7	-70.5			199.8	544.7	115.8	9.6	1.000044
52500.0	112.[illegible]	-70.[illegible]			193.9	544.5	116.9	11.0	1.000043
53000.0	109.9	-70.7			189.1	544.3	115.6	11.6	1.000042
53500.0	107.1	-70.8			184.5	544.1	114.[illegible]	12.2	1.000041
54000.0	104.[illegible]	-71.0			179.9	543.9	115.3	12.8	1.000040
54500.0	101.[illegible]	-71.1			175.5	543.8	115.9	13.5	1.000039
55000.0	99.[illegible]	-70.[illegible]			170.9	544.1	117.7	14.9	1.000038
55500.0	96.[illegible]	-69.7			165.7	545.7	119.2	15.1	1.000037
56000.0	94.[illegible]	-68.5			160.7	547.3	120.6	15.[illegible]	1.000036
56500.0	92.[illegible]	-67.4			155.8	548.9	122.0	15.0	1.000035
57000.0	89.7	-66.2			151.1	549.6	123.0	14.2	1.000034
57500.0	87.[illegible]	-65.0			146.5	552.0	124.0	13.3	1.000033
58000.0	85.[illegible]	-63.[illegible]			142.1	553.6	125.2	11.6	1.000032
58500.0	83.3	-63.[illegible]			139.5	553.5	124.5	9.8	1.000031
59000.0	81.[illegible]	-64.0			135.3	553.4	102.[illegible]	7.7	1.000030
59500.0	79.[illegible]	-64.1			132.1	553.2	75.2	7.8	1.000029
60000.0	77.[illegible]	-64.2			129.2	553.1	76.2	13.1	1.000029
60500.0	75.4	-64.[illegible]			125.9	552.9	77.1	18.3	1.000028
61000.0	73.[illegible]	-64.5			122.3	552.8	83.4	21.9	1.000027
61500.0	71.[illegible]	-64.6			119.9	552.6	88.2	25.6	1.000027
62000.0	70.0	-64.7			117.0	552.5	94.1	24.9	1.000026
62500.0	68.[illegible]	-64.[illegible]			113.9	553.1	100.3	24.6	1.000025
63000.0	66.6	-63.8			110.9	553.7	103.5	24.5	1.000025

STATION ALTITUDE 3909.00 FEET MSL
6 JULY 84 0900 HRS MST
ASCENSION NO. 256

UPPER AIR DATA
1980 20355
WHITE SANDS

GEODETIC COORDINATES
32.63043 LAT DEG
106.37933 LON DEG

GEOMETRIC ALTITUDE MSL FEET	PRESSURE MILLIBARS	TEMPERATURE AIR DEGREES CENTIGRADE	TEMPERATURE DEWPOINT CENTIGRADE	REL.HUM. PERCENT	DENSITY GM/CUBIC METER	SPEED OF SOUND KNOTS	WIND DATA DIRECTION DEGREES(TN)	WIND DATA SPEED KNOTS	INDEX OF REFRACTION
63500.0	65.0	-43.3			108.3	564.3	106.2	24.5	1.000024
64000.0	63.4	-42.7			105.1	564.9	106.1	24.7	1.000023
64500.0	61.9	-42.4			102.3	565.6	103.9	25.2	1.000023
65000.0	60.4	-41.9			99.5	566.2	99.9	25.6	1.000022
65500.0	58.9	-41.5			97.0	566.8	93.7	26.2	1.000022
66000.0	57.5	-40.9			94.4	567.6	87.2	27.4	1.000021
66500.0	56.1	-40.1			91.8	568.6	81.4	27.5	1.000020
67000.0	54.8	-39.4			89.3	569.5	81.5	27.6	1.000020
67500.0	53.5	-38.7			86.9	570.5	86.3	26.8	1.000019
68000.0	52.2	-38.0			84.5	571.4	94.4	26.0	1.000019
68500.0	51.0	-37.3			82.3	572.4	99.7	25.8	1.000018
69000.0	49.8	-36.8			80.1	573.1	99.2	26.0	1.000018
69500.0	48.6	-37.0			78.3	572.7	98.7	26.3	1.000017
70000.0	47.4	-37.2			76.5	572.3	98.5	26.2	1.000017
70500.0	46.3	-37.6			74.9	571.9	98.3	26.0	1.000017
71000.0	45.2	-37.9			73.2	571.5	98.1	26.0	1.000016
71500.0	44.2	-37.9			71.5	571.6	98.0	25.9	1.000016
72000.0	43.1	-37.3			69.5	572.4	97.9	25.9	1.000015
72500.0	42.1	-36.7			67.8	573.2	101.5	25.7	1.000015
73000.0	41.1	-36.1			66.0	573.9	105.2	25.6	1.000015
73500.0	40.2	-35.5			64.3	574.7	106.5	25.5	1.000014
74000.0	39.2	-35.0			62.5	575.5	106.7	24.0	1.000014
74500.0	38.3	-34.4			61.0	575.2	105.8	25.3	1.000014
75000.0	37.4	-33.8			59.4	577.0	102.7	23.5	1.000013
75500.0	36.5	-33.2			57.9	577.7	99.5	23.7	1.000013
76000.0	35.7	-32.8			56.4	578.3	99.7	24.5	1.000013
76500.0	34.8	-32.9			55.1	578.2	99.8	25.4	1.000012
77000.0	34.0	-33.0			53.9	578.1	99.4	25.2	1.000012
77500.0	33.2	-33.1			52.6	578.0	97.9	25.3	1.000012
78000.0	32.5	-33.1			51.6	577.9	96.7	21.5	1.000011
78500.0	31.7	-33.2			50.2	577.8	95.0	20.8	1.000011
79000.0	31.0	-33.3			49.1	577.7	96.3	20.9	1.000011
79500.0	30.2	-33.4			48.0	577.5	96.9	20.9	1.000011
80000.0	29.6	-33.3			46.9	577.7	95.4	22.3	1.000010
80500.0	28.9	-33.1			45.7	577.9	97.3	23.8	1.000010
81000.0	28.2	-32.9			44.5	578.1	92.5	25.3	1.000010
81500.0	27.6	-32.8			43.5	578.4	88.4	25.6	1.000010
82000.0	26.9	-32.6			42.5	578.6	84.4	29.1	1.000009
82500.0	26.3	-32.4			41.5	578.8	81.8	29.7	1.000009
83000.0	25.7	-32.2			40.5	579.1	83.2	32.5	1.000009

UPPER AIR DATA
19[illegible]2366
WHITE SANDS

STATION ALTITUDE 3[illegible]9.0 FEET MSL
6 JULY 8[illegible] [illegible]600 HRS MST
ASCENSION NO. [illegible]56

GEODETIC COORDINATES
32.40043 LAT DEG
106.37033 LON DEG

GEOMETRIC ALTITUDE MSL FEET	PRESSURE MILLIBARS	TEMPERATURE AIR DEGREES CENTIGRADE	TEMPERATURE DEWPOINT DEGREES CENTIGRADE	REL.HUM. PERCENT	DENSITY GM/CUBIC METER	SPEED OF SOUND KNOTS	WIND DATA DIRECTION DEGREES(TN)	WIND DATA SPEED KNOTS	INDEX OF REFRACTION
3[illegible]560.0	[illegible]5.1	-[illegible]2.[illegible]			39.5	579.3	94.4	35.[illegible]	1.[illegible]
94000.0	[illegible]4.5	-51.9			39.5	579.5	85.4	37.9	1.000009
94500.0	24.[illegible]	-[illegible]1.6			37.7	579.8	86.5	40.1	1.000005
95000.0	23.4	-50.9			36.7	580.7	87.5	42.2	1.000008
95500.0	22.9	-[illegible]0.2			35.8	581.7	88.0	43.9	1.000005
96000.0	[illegible]2.4	-49.[illegible]			34.8	582.6	87.4	44.[illegible]	1.000008
96500.0	21.9	-48.[illegible]			33.9	583.5	86.9	44.8	1.000005
97000.0	[illegible]1.[illegible]	-47.1			33.1	584.4	86.5	45.4	1.000007
97500.0	20.9	-47.[illegible]			32.2	585.3	86.3	46.0	1.000007
98000.0	[illegible]0.4	-46.7			31.4	586.2	86.1	46.7	1.000007
98500.0	19.9	-46.0			30.6	587.1	86.1	47.3	1.000007
99000.0	19.5	-45.6			29.8	587.7	85.2	47.9	1.000007
99500.0	19.1	-45.[illegible]			29.1	588.2	86.3	48.5	1.000006
100000.0	18.[illegible]	-44.6			28.4	588.7	86.1	48.3	1.000006
100500.0	18.[illegible]	-44.3			27.7	589.3	85.3	47.0	1.000006
101000.0	17.[illegible]	-43.9			27.1	589.8	84.6	45.7	1.000006
101500.0	17.4	-43.5			26.4	590.4	84.2	44.9	1.000006
102000.0	17.0	-43.1			25.8	590.9	84.5	45.3	1.000006
102500.0	16.6	-42.7			25.2	591.5	84.9	45.6	1.000006
103000.0	16.[illegible]	-42.[illegible]			24.6	591.7	85.6	46.0	1.000006
103500.0	15.9	-42.2			24.0	592.0	87.7	45.4	1.000005
104000.0	15.6	-42.1			23.5	592.2	89.8	45.8	1.000006
104500.0	15.2	-41.9			22.9	592.5	91.8	47.4	1.000006
105000.0	14.9	-41.7			22.4	592.7	93.7	45.7	1.000006
105500.0	14.6	-41.5			21.9	593.0	94.6	45.8	1.000005
106000.0	14.[illegible]	-41.3			21.4	593.2	96.0	44.9	1.000006
106500.0	13.9	-41.1			20.9	593.5			1.000006
107000.0	13.6	-40.9			20.4	593.7			1.000006
107500.0	13.[illegible]	-40.7			20.0	593.9			1.000004
108000.0	13.[illegible]	-40.5			19.5	594.2			1.000004
108500.0	12.7	-40.3			19.1	594.4			1.000004
109000.0	12.5	-40.1			18.6	594.7			1.000004

RAW SIGNIFICANT LEVEL DATA

STATION ALTITUDE 3989.00 FEET MSL
8 JULY 84 0815 HRS MST
ASCENSION NO. 586

1000370366
WHITE SANDS

GEODETIC COORDINATES
32.45043 LAT DEG
106.37033 LON DEG

GEOPOTENTIAL ALTITUDE DECAMETERS	WIND DATA DIRECTION DEG (TN)	WIND DATA SPEED MPS	WIND DATA N-S MPS	WIND DATA E-W MPS	DEW PT DEP DEG C	TEMPERATURE AIR DEG C	PRESSURE MILLIBARS
3035.	9999.**	9999.**	-9999.**	-9999.**	99	-40.1	1.240+1
3057.	85.	2.	-2.	-2.	99	-42.5	1.650+1
2962.	86.	24.	-2.	-24.	99	-45.1	2.000+1
2563.	86.	21.	-1.	-21.	99	-51.7	2.490+1
2419.	94.	11.	1.	-11.	99	-53.4	3.000+1
2303.	100.	13.	2.	-12.	99	-52.8	3.590+1
2164.	98.	13.	2.	-13.	99	-53.1	4.450+1
2092.	99.	13.	2.	-13.	99	-56.7	5.000+1
1995.	87.	14.	-1.	-14.	99	-51.3	5.840+1
1953.	94.	13.	1.	-13.	99	-54.7	7.000+1
1753.	125.	6.	3.	-5.	99	-53.8	8.520+1
1667.	117.	7.	3.	-7.	99	-71.2	1.000+2

** WIND DATA NOT COMPUTED DUE TO MISSING RAW AZIMUTH AND ELEVATION ANGLES.

STATION ALTITUDE 3939.0 FEET MSL
6 JULY 64 0800 HRS MST
ASCENSION NO. 366

MANDATORY LEVELS
1*0333*66
WHITE SANDS

GEODETIC COORDINATES
32.43043 LAT DEG
106.37733 LON DEG

PRESSURE MILLIBARS	GEOPOTENTIAL FEET	TEMPERATURE AIR DEGREES CENTIGRADE	TEMPERATURE DEWPOINT CENTIGRADE	REL.HUM. PERCENT	WIND DATA DIRECTION DEGREES(TN)	WIND DATA SPEED KNOTS
693.0	5015.	22.7	9.1	42.	190.9	7.1
700.0	6747.	20.2	7.6	44.	193.9	10.8
750.0	8555.	16.1	5.3	49.	206.4	7.0
700.0	10467.	11.5	2.5	54.	126.9	6.5
650.0	12481.	6.1	-.5	53.	54.1	12.3
600.0	14617.	2.5	-14.7	27.	101.1	13.4
550.0	16911.	-.8	-21.5	19.	137.4	15.7
500.0	19389.	-7.1	-26.7	19.	143.7	14.6
450.0	22065.	-10.5	-30.0	18.	152.7	19.8
400.0	25007.	-17.0	-34.1	21.	150.4	15.3
350.0	28243.	-23.5	-40.9	20.	147.8	10.2
300.0	31875.	-33.3	-48.9	21.	92.5	4.6
250.0	35999.	-42.9			22.5	9.1
200.0	40911.	-53.9			358.4	17.7
175.0	43539.	-59.5			341.2	8.6
150.0	46717.	-64.9			27.3	14.9
125.0	50335.	-69.2			90.8	6.5
100.0	54477.	-71.2			117.1	14.4
80.0	59189.	-64.1			66.1	7.5
70.0	61789.	-64.7			93.3	25.0
60.0	64997.	-61.8			99.1	25.6
50.0	68642.	-56.7			99.4	26.0
40.0	73275.	-55.4			105.5	24.9
30.0	79348.	-53.6			94.5	21.2
25.0	83211.	-52.0			84.5	35.5
20.0	86063.	-46.1			86.7	47.2
15.0	94355.	-41.7			92.7	47.1

** AT LEAST ONE ASSUMED RELATIVE HUMIDITY VALUE WAS USED IN THE INTERPOLATION.

MRN MANDATORY LEVELS

STATION ALTITUDE 1989.0 FEET MSL
8 JULY 84 0300 HRS MST
ASCENSION NO. 355

1989?3366
WHITE SANDS

GEODETIC COORDINATES
32.40843 LAT DEG
106.37033 LON DEG

GEOPOTENTIAL ALTITUDE DECAMETERS	WIND DATA DIRECTION DEG (TN)	SPEED MPS	N-S MPS	E-W MPS	DEW PT DEP DEG C	TEMPERATURE AIR DEG C	PRESSURE MILLIBARS
2876.	9?.	24.	1.	-24.	99	-41.7	1.500+1
2652.	84.	24.	-2.	-24.	99	-44.1	2.000+1
2536.	84.	13.	-2.	-12.	99	-52.1	2.500+1
2419.	97.	11.	1.	-11.	99	-53.4	3.000+1
2233.	107.	13.	4.	-12.	99	-55.4	4.000+1
2092.	9?.	12.	2.	-12.	99	-56.7	5.000+1
1978.	9?.	13.	2.	-13.	99	-61.8	6.000+1
1883.	94.	12.	1.	-12.	99	-64.7	7.000+1
1802.	86.	4.	-0.	-4.	99	-64.1	8.000+1
1687.	117.	7.	3.	-7.	99	-71.2	1.000+2
1534.	91.	7.	0.	-7.	99	-69.2	1.250+2
1424.	27.	9.	-7.	-4.	99	-56.0	1.500+2
1329.	341.	4.	-4.	1.	99	-59.5	1.750+2
1244.	359.	9.	-9.	0.	99	-53.9	2.000+2
1097.	27.	5.	-4.	-2.	99	-42.9	2.500+2
972.	93.	7.	0.	-2.	15	-33.3	3.000+2
881.	148.	5.	4.	-3.	17	-27.5	3.500+2
782.	150.	8.	7.	-4.	17	-17.0	4.000+2
673.	163.	10.	10.	-3.	19	-11.5	4.500+2
591.	144.	7.	6.	-4.	20	-7.1	5.000+2
515.	133.	9.	6.	-6.	21	-.8	5.500+2
446.	101.	7.	1.	-7.	17	2.5	6.000+2
380.	84.	5.	-1.	-5.	17	5.1	6.500+2
319.	125.	3.	1.	-2.	99	11.5	7.000+2
261.	206.	4.	-1.	2.	11	15.1	7.500+2
205.	194.	6.	5.	1.	13	20.2	8.000+2
153.	191.	6.	4.	1.	14	22.7	8.500+2